Chapter 3

USP11 Counteracts RNF4 and Stabilizes PML Nuclear Bodies

Ivo A. Hendriks[1*], Joost Schimmel[1*], Jesper V. Olsen[2] and Alfred C.O. Vertegaal[1]

[1]Department of Molecular Cell Biology, Leiden University Medical Center, Albinusdreef 2, 2333 ZA, Leiden, the Netherlands
[2]Novo Nordisk Foundation Center for Protein Research, Faculty of Health and Medical Sciences, University of Copenhagen, Blegdamsvej 3B, 2200 Copenhagen, Denmark.
[*]These authors contributed equally to this work

Chapter 3 has been submitted for publication

3

ABSTRACT

RNF4 is a SUMO-targeted ubiquitin E3 ligase, with a pivotal function in the DNA damage response (DDR). We identified the deubiquitylating enzyme USP11, a known DDR-component, as an interactor of RNF4. USP11 can deubiquitylate hybrid SUMO-ubiquitin chains to counteract RNF4. Four closely spaced SUMO Interacting Motifs (SIMs) in USP11 are required for its activity, revealing USP11 as a SUMO-targeted ubiquitin protease. SUMO-enriched nuclear bodies are stabilized by USP11, which functions downstream of RNF4 as a counterbalancing mechanism. In response to DNA damage induced by methyl methanesulfonate, USP11 counteracts RNF4 to block the dissolution of nuclear bodies. Thus, we provide novel insight into crosstalk between ubiquitin in SUMO, and uncover USP11 and RNF4 as a balanced SUMO-targeted ubiquitin ligase/protease pair with a role in the DDR.

INTRODUCTION

Small Ubiquitin-like Modifiers (SUMOs) are predominantly located in the nucleus and play key roles in all nuclear processes including transcription, chromatin modification and maintenance of genome stability [1]. Analogous to the ubiquitin system, a set of E1, E2 and E3 enzymes mediate the conjugation of SUMO to target proteins, and a set of SUMO-specific proteases is responsible for the reversible nature of this post-translational modification [2, 3]. Mouse models have shown that the SUMOylation system is essential for embryonic development. Mice deficient for the single SUMO E2 enzyme Ubc9 die at the early post-implantation stage as a result of hypocondensation and other chromosomal aberrancies [4].

Large sets of target proteins have been identified for the different SUMO family members, involved in all different nuclear processes [5-7]. About half of the SUMO acceptor lysines in these target proteins are located in short stretches that fit the SUMOylation consensus motif ΨKxE [7, 8], a motif that is directly recognized by Ubc9 [9, 10]. SUMO signal transduction furthermore includes proteins that bind non-covalently to SUMOylated proteins via SUMO-Interaction Motifs (SIMs) [11], including the novel SUMO-binding Zinc finger identified in HERC2 [12].

Interestingly, extensive crosstalk exists between the SUMOylation system and the ubiquitylation system [13, 14]. This crosstalk includes competition between SUMO and ubiquitin for the same acceptor lysines [15], or sequential modification by SUMO and ubiquitin of a target protein [16]. Moreover, the SUMO system is tightly connected to the ubiquitin-proteasome pathway since a significant subset of SUMO-2/3 target proteins is subsequently ubiquitylated and degraded by the proteasome [17, 18]. Inhibition of the proteasome led to accumulation of SUMO-2/3 conjugates and the depletion of the pool of non-conjugated SUMO-2/3, indicating that this biochemical pathway is required for SUMO-2/3 recycling. SUMO and ubiquitin can form hybrid chains, including via lysine 32 of SUMO-2 or lysine 33 of SUMO-3 [17].

The SUMO system and the ubiquitin system are linked together via the SUMO-targeted ubiquitin ligases (STUbLs), responsible for ubiquitylating SUMOylated proteins. They were first identified in *Schizosacharomyces pombe* as Rfp1 and Rfp2 and in *Saccharomyces cerevisiae* as the Slx5-Slx8 complex [19, 20]. Rfp1 and -2 each have an N-terminal SIM and a C-terminal RING-finger domain to enable interaction with SUMOylated proteins. Ubiquitin E3 ligase activity is obtained by RING-RING-mediated recruitment of the active RING-finger protein Slx8. RNF4 is a major mammalian STUbL containing four N-terminal SIMs and a C-terminal RING domain that enables homodimerization [21]. More recently, RNF111/Arkadia was identified as a second mammalian STUbL [22, 23].

STUbLs play key roles in the DNA damage response [24]. *Schizosacharomyces pombe* strains deficient for STUbLs display genomic instability and are hypersensitive to different DNA damaging agents including hydroxyurea (HU), methylmethane

sulfonate (MMS), camptothecin (CPT) and ultraviolet (UV) light [19, 20]. RNF4 knockdown in human cells also results in increased sensitivity to DNA-damaging agents [25]. Moreover, RNF4 accumulates at DNA damage sites induced by laser micro-irradiation [25-27]. SUMOylated target proteins for RNF4 include MDC1 and BRCA1 [27, 28] and furthermore HIF-2α [29]. Mice deficient for RNF4 die during embryogenesis [27, 30]. Mice expressing strongly reduced levels of RNF4 are born alive, albeit at a reduced Mendelian ratio, and showed an age-dependent impairment in spermatogenesis [27]. MEFs derived from these mice exhibit increased sensitivity to genotoxic stress.

A key feature of ubiquitin-like modification systems is their reversible nature to carefully balance cellular systems [2, 31]. Deubiquitylating enzymes (DUBs) play a pivotal role in the regulation of cellular ubiquitylation levels, essentially controlling all cellular processes. There are around 100 DUBs, with different substrate specificity, subcellular localization, and protein-protein interactions [31, 32]. Currently, it is not clear how the activity of the STUbLs is balanced. Here, we report the identification of a ubiquitin-specific protease with the ability to counteract RNF4.

RESULTS

Purification of FLAG-tagged Ring Finger Protein 4 (RNF4) from MCF7 cells

SUMO-targeted ubiquitin ligase RNF4 specifically recognizes targets that are modified by multiple SUMOs, through recognition of the SUMO-fold with its SUMOylation Interacting Motifs (SIMs) [11, 33]. Subsequently, these SUMOylated targets are ubiquitylated by RNF4, which can lead to the degradation of these proteins by the proteasome [21, 34, 35]. Poly-SUMOylated targets of RNF4 have been identified employing a trap consisting of the RNF4 SIM-domain [36].

We were interested in identifying SIM-independent RNF4 interactors. In order to facilitate this study, an MCF7 cell line stably expressing C-terminally FLAG-tagged RNF4 was generated, and a biological triplicate experiment comparing the parental MCF7 cell line versus the RNF4-FLAG cell line was performed. The levels of RNF4-FLAG in all experiments were investigated following lysis of the cells (**Figure 1A and 1B**). Relative to the endogenous RNF4, there is a moderate overexpression of RNF4-FLAG. Considering the highly specific nature of the FLAG antibody, and the exploratory nature of our experiment, such expression levels are acceptable. The subcellular localization of RNF4-FLAG was inspected by confocal fluorescent microscopy, demonstrating the fusion protein to be located correctly and exclusively in the nucleus (**Figure 1C**). Some of the RNF4-FLAG localized into nuclear bodies, which likely correspond to PML nuclear bodies. The non-fused and co-expressing Green Fluorescent Protein (GFP) was included as a control.

We performed FLAG-immunoprecipitation (IP), and found that RNF4-FLAG is very efficiently purified, with no other signal other than RNF4-FLAG being detectable by immunoblot (**Figure 1D**). Lysis of the cells and IP of FLAG was performed

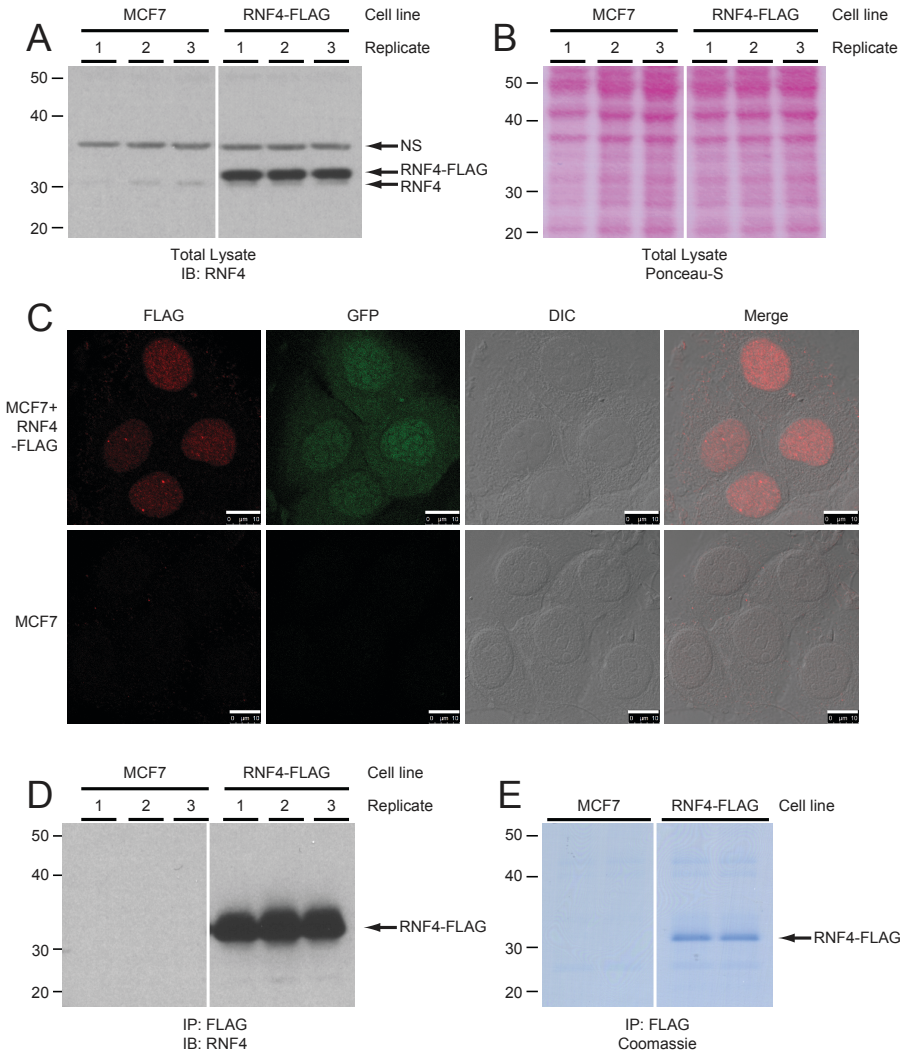

Figure 1. Generation of a cell line stably expressing RNF4-FLAG.

A) MCF7 cells were infected with a bicistronic lentivirus encoding RNF4-FLAG and GFP separated by an Internal Ribosome Entry Site (IRES). Cells stably expressing low levels of the transgene were selected by flow cytometry. Total lysates were analyzed by immunoblotting to confirm expression of RNF4-FLAG relative to endogenous RNF4. The experiment was performed in biological triplicate for mass spectrometric analysis.

B) Ponceau-S loading control for section A.

C) Stable cell lines were investigated by confocal fluorescent microscopy to confirm the nuclear localization of RNF4-FLAG. GFP was visualized as an expression control, and differential interference contrast (DIC) was used to localize the cellular nuclei. Scale bars represent 10 µm.

D) RNF4 complexes were purified by immunoprecipitation (IP), and three biological replicates were analyzed by immunoblotting (IB) for the presence of RNF4. Parental cells were included as a negative control.

E) Coomassie analysis of one replicate of the FLAG-IP, loaded over two lanes, prior to in-gel digestion and analysis by LC-MS/MS.

A

Protein	USP11		RNF4	
Cell line	MCF7	RNF4	MCF7	RNF4
Unique Peptides	2	12	1	11
LFQ Intensity (10log)	3.3	5.6	3.8	7.4
MS/MS Count	0	11	0	26
LFQ Ratio (2log)	5.1		10.8	

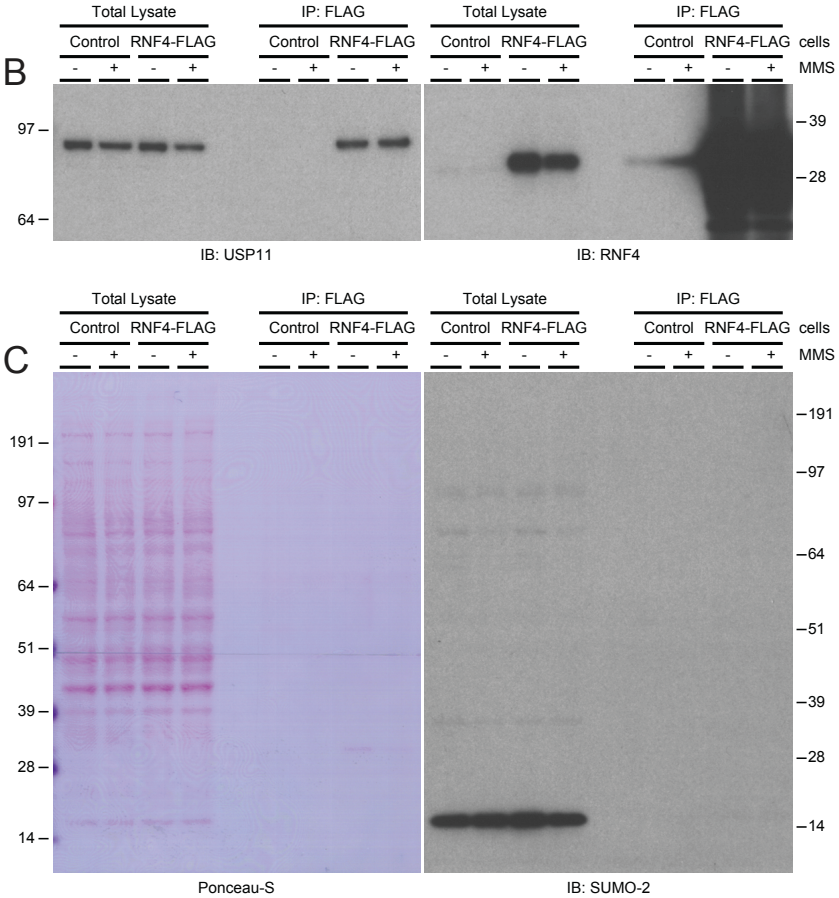

Figure 2. Identification of USP11 as an RNF4-interacting ubiquitin protease.

A) Overview of the mass spectrometry results pertaining to USP11 and RNF4. USP11 was found to be significantly enriched after FLAG-IP from the RNF4-FLAG stable cell line, with 0/0/0 USP11 MS/MS counts in the parental line versus 8/14/11 USP11 MS/MS counts in the RNF4-FLAG line, respectively. USP11 was found to be enriched after RNF4-FLAG IP with a Label-Free Quantification (LFQ) Log_2 ratio of over 5.

B) MCF7 cell lines expressing RNF4-FLAG and parental controls were treated with methyl methanesulfonate (MMS), lysed, and FLAG-IP was performed. Total lysates and IP fractions were analyzed by immunoblotting against USP11 to confirm the co-immunoprecipitation of endogenous USP11 with RNF4-FLAG. Immunoblotting for RNF4 was performed as an immunoprecipitation control.

C) Ponceau-S loading control for section B. Additionally, total lysates and IP fractions were analyzed by immunoblotting against SUMO-2 to investigate potential co-immunoprecipitation of SUMO-2 with RNF4 through its SUMO-interacting motifs (SIMs).

under relatively stringent conditions, but mild enough for the robust SUMO-specific proteases (SENPs) to still be able to cleave SUMO off all target proteins. Finally, prior to in-gel digestion and LC-MS/MS analysis, Coomassie analysis of the purified RNF4-FLAG and its potential interactors revealed a singular and very clear band corresponding to RNF4-FLAG, indicative of a clean and highly stringent purification of RNF4-FLAG (**Figure 1E**).

Identification of Ubiquitin-Specific Protease 11 (USP11) as an Interactor of RNF4

The RNF4-FLAG IP was performed in biological triplicate, and the gel lanes were cut in five separate slices and analyzed by mass spectrometry experiments. Over 800 proteins were identified in the FLAG-IP samples, with nearly all of these proteins being background proteins equally identified in the RNF4-FLAG line and the parental control. Only a few proteins were specifically and significantly enriched in the RNF4-FLAG line, indicatory of the stringent purification conditions. Strikingly, we did not detect free or conjugated forms of SUMO in the IP, proving that our lysis and IP conditions were sufficiently harsh to yield a clean IP, yet mild enough to allow the highly robust SENPs to cleave SUMO off virtually all proteins. Unsurprisingly, RNF4 itself was detected as the highest enriching protein after RNF4-FLAG IP. Furthermore, we identified the ubiquitin carboxyl-terminal hydrolase 11 (USP11) as an important RNF4 interactor (**Figure 2A**), as USP11's innate function as a ubiquitin protease is directly opposing of RNF4's function as a ubiquitin ligase. USP11 was found to be enriched over the control with a Log_2 ratio of 5.1, and eleven MS/MS spectral identifications matching USP11 were made in the RNF4-FLAG IP as opposed to zero in the control IP.

After finding USP11 as an interactor of RNF4 through mass spectrometry analysis, the experiment was repeated, and samples were analyzed by immunoblotting (**Figure 2B**). Additionally, a potential effect of the DNA damaging agent methyl methanesulfonate (MMS) on the interaction between RNF4 and USP11 was investigated, as MMS is known to cause disassembly of the PML nuclear bodies harboring RNF4 [37]. After RNF4-FLAG IP, immunoblot analysis with an antibody against endogenous USP11 shows a very clear and specific interaction with RNF4, with no signal detectable in the parental control (**Figure 2B**). There was no indication that the interaction between RNF4 and USP11 is disrupted upon treating the cells with MMS. A small decrease in both RNF4 and USP11 levels was observed after DNA damage, indicative of their function in the DNA damage response, which may eventually lead to their degradation. Even though input levels of both RNF4-FLAG and USP11 dropped slightly after MMS treatment, the detectable level of USP11 co-immunoprecipitating with RNF4 remains identical. Finally, equal protein loading was validated through Ponceau-S staining, and immunoblot analysis with an antibody against SUMO-2 was performed to investigate the SUMOylation state of proteins in the total lysate and the IP fractions (**Figure 2C**). In agreement with the mass spectrometry findings, free SUMO was detected only in the total lysates, a direct result

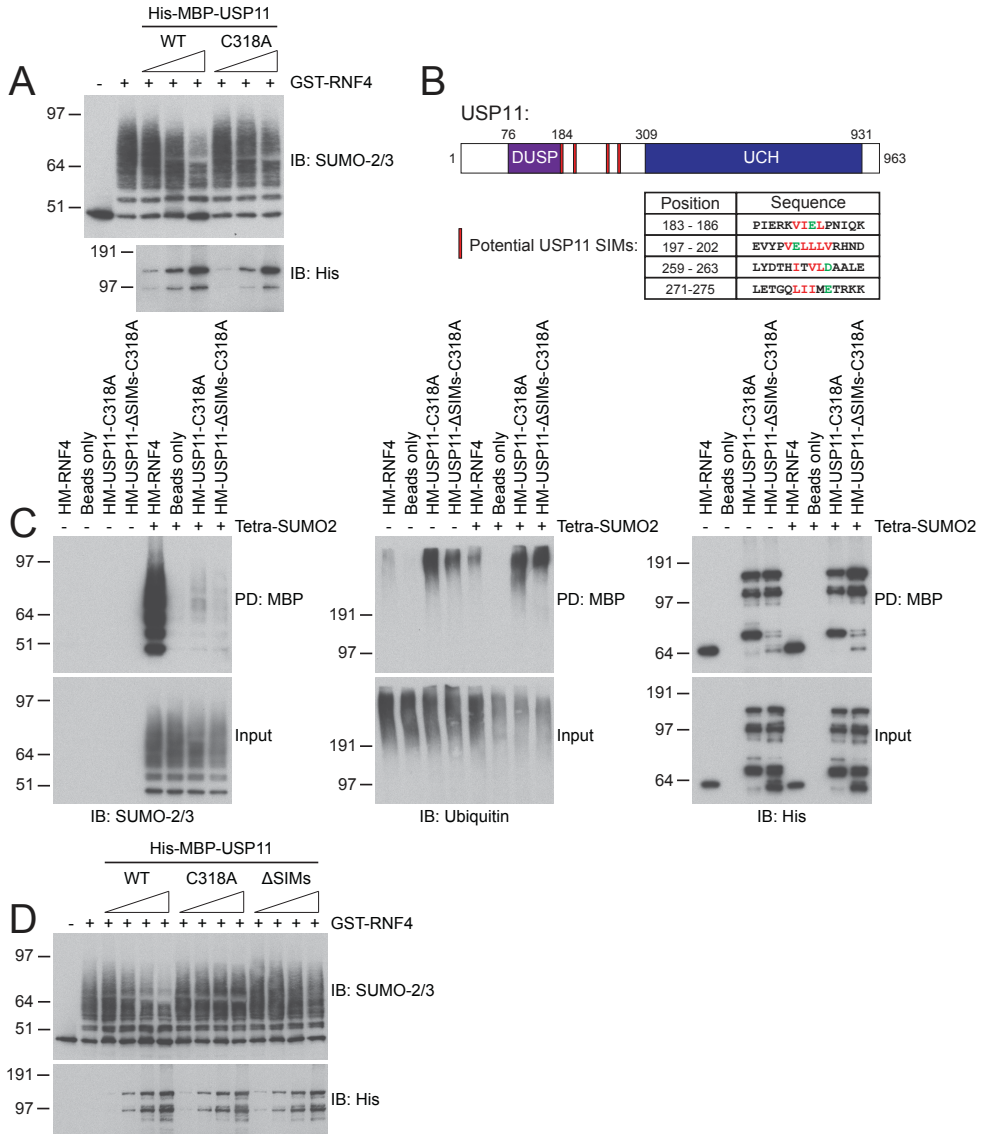

Figure 3. USP11 deubiquitylates hybrid SUMO-2-ubiquitin chains *in vitro* in a SIM-dependent manner.

A) His_6-tetra-SUMO-2 proteins were *in vitro* ubiquitylated by GST-RNF4. The resulting SUMO-ubiquitin hybrid chains were incubated with increasing concentrations of His_6-MBP-USP11 wild-type (WT) or a catalytic inactive mutant (C318A). Hybrid chains were analyzed by immunoblotting against SUMO-2/3 and His_6-MBP-USP11 levels were analyzed by immunoblotting against the poly-Histidine tag (anti-His).

B) Cartoon depicting USP11. USP11 harbors a Domain present in Ubiquitin-Specific Proteases (DUSP) and an Ubiquitin Carboxyl-terminal Hydrolase domain (UCH). USP11 contains four potential SUMO interacting motifs (SIMs), located in between the DUSP and UCH domains. Hydrophobic residues depicted in red were incubated replace by alanines to generate a USP11 ΔSIM mutant.

of the SENPs removing all SUMO from target proteins following lysis, indicating that the interaction between USP11 and RNF4 is SUMOylation-independent.

USP11 deubiquitylates SUMO-2-ubiquitin hybrid chains *in vitro* in a SIM-dependent manner

To test whether USP11 can counteract RNF4 *in vitro*, a hybrid SUMO-2-ubiquitin polymer was generated as a potential USP11 substrate, using a recombinant linear SUMO-2 polymer, composed of four SUMO proteins which was ubiquitylated *in vitro* by RNF4 [21]. Subsequently, recombinant USP11 was added to the reaction to analyze the deubiquitylation activity of USP11. Adding wild type USP11 resulted in the deubiquitylation of SUMO-2-ubiquitin hybrid chains while adding a catalytic inactive USP11 mutant (C318A) had no effect on these chains (**Figure 3A**). Since USP11 and RNF4 were simultaneously present in the reaction mixture, a limited amount of ubiquitylated SUMO-2 polymer was still detected, probably representing multiple mono-ubiquitylated forms. We conclude that USP11 could indeed counteract the activity of RNF4 on a SUMO-2 polymer *in vitro*.

Analysis of the USP11 sequence revealed four potential SIMs located in an undefined domain between the DUSP and UCH domains of USP11 (**Figure 3B**). To further establish confidence in these SIMs, PHYRE2 [38] was used to generate a structural model of USP11 (**Figure S1A**). Using homology modeling and superimposition of multiple homologous known structural elements, a USP11 structure was generated with 65% of residues modeled at 90% or greater confidence. 283 out of 931 residues could not be aligned to existing structures, and were modeled *ab initio*. These residues were mainly located within the center of the UCH. The four potential SIMs in USP11 (**Figure 3B and S1B**) were observed to be located on a "bridge" connecting the DUSP with the UCH domains in a clustered manner to enable synergistic binding to SUMO polymers (**Figure S1C**). All of the SIMs were solvent-exposed, and located in a region of USP11 accessible for small proteins such as SUMO or ubiquitin.

A USP11 mutant lacking SIMs (ΔSIMs) was generated by mutating the large hydrophobic residues in the SIMs to alanines. Note that this mutant was made in the background of the C318A mutant to prevent deubiquitylation activity on the chains during the interaction experiments. To analyze the interaction between USP11 and

C) Ubiquitin chains only (-) or SUMO-2-Ubiquitin mixed chains (+) were incubated with His_6-MBP(HM)-RNF4, His_6-MBP(HM)-USP11-C318A, or His_6-MBP(HM)-USP11-C318A proteins where the four potential SIMs were mutated (ΔSIMs-C318A). His_6-MBP proteins were subsequently purified with amylose beads to enrich for the MBP tag. Amylose beads-only samples were used as a negative control. Inputs and bound proteins were analyzed by immunoblotting with the indicated antibodies.

D) The experiment described in section A was repeated and the His-MBP-USP11-ΔSIMs protein was included to study the contribution of the SIMs.

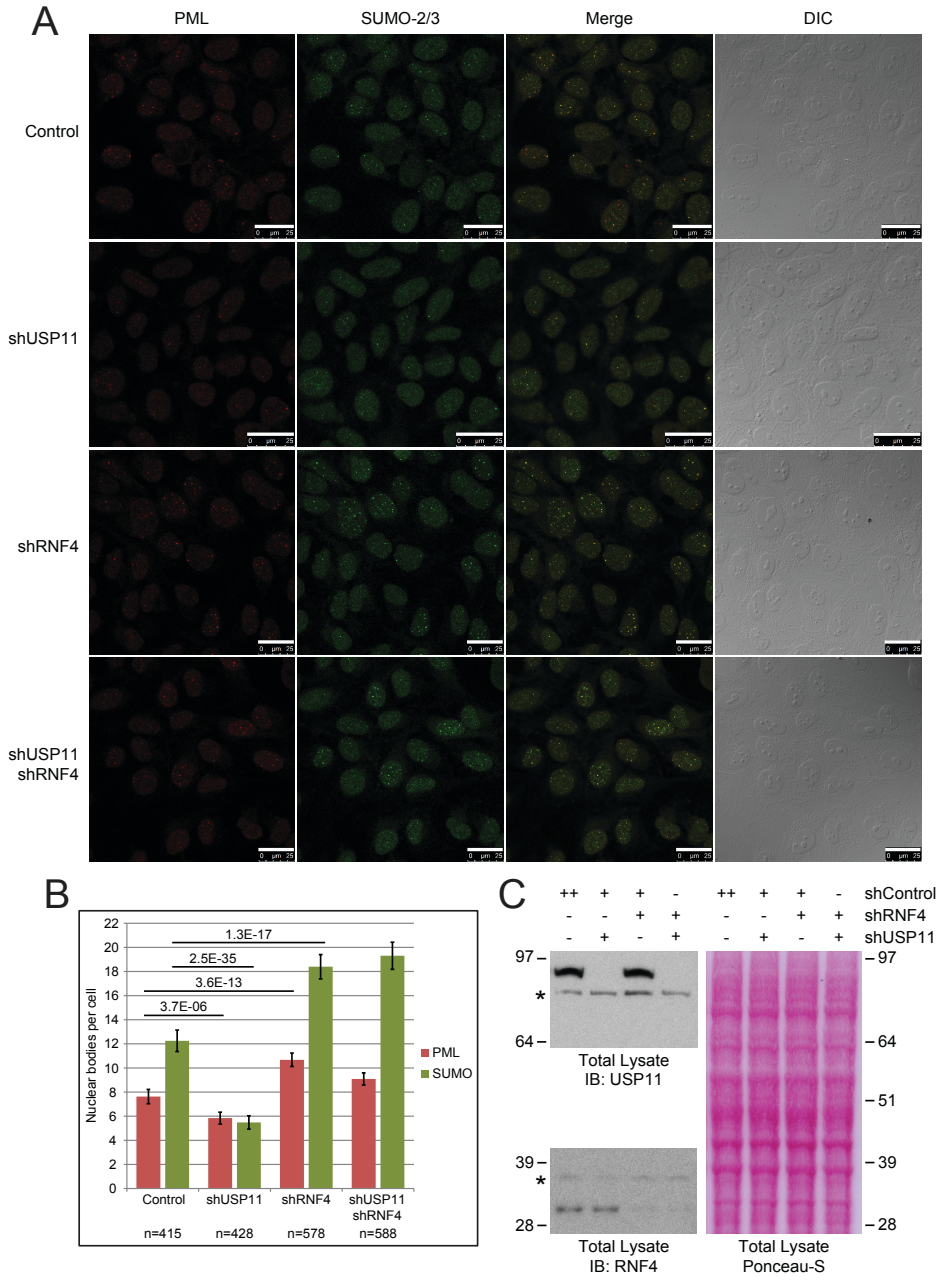

Figure 4. USP11 stabilizes PML and SUMO nuclear bodies, counteracting the destabilizing effect of RNF4.

A) U2OS cells were depleted for endogenous USP11, RNF4, or both, by infection with lentiviral knockdown constructs. As a control, an untargeted lentiviral knockdown construct was used. Following depletion of proteins, cells were fixed, immunostained and subsequently analyzed by confocal fluorescence microscopy for the presence of PML and SUMO-2/3 positive nuclear bodies. Images represent maximum projections of Z-stacks. DIC was used to visualize the nuclei. Depletion

SUMO-2 and/or ubiquitin, the SUMO-Ubiquitin mixed chains described above or unanchored ubiquitin chains made by RNF4 were used. SUMO-2/3 immunoblot analysis confirmed the strong interaction between RNF4 and SUMO-2-Ubiquitin mixed chains. Compared to RNF4, USP11 displayed a weak but visible interaction with these mixed chains and this interaction was reduced by mutating the SIMs of USP11 (**Figure 3C**). In contrast, USP11 had more affinity for binding unanchored ubiquitin chains as compared to RNF4 (**Figure 3C**).

Interestingly, mutating these four SIMs in USP11 prevented the processing of these hybrid chains, indicating that USP11 deubiquitylates SUMO-ubiquitin hybrids in a SIM-dependent manner (**Figure 3D**).

USP11 counterbalances RNF4 and controls stability of nuclear bodies

Since RNF4 is known to ubiquitylate SUMOylated PML, which in turn leads to degradation of PML and the destabilization of nuclear bodies [21], we set out to study the role of endogenous USP11 in nuclear body integrity. Lentiviral shRNA-mediated depletion of endogenous USP11 or RNF4, or depletion of both proteins was performed, prior to analysis of the cells by confocal Z-stacked fluorescent microscopy (**Figure 4A**). The effect on PML bodies and additionally the effect on other SUMO nuclear bodies was investigated. Although SUMO and PML can co-localize in nuclear bodies, the overlap is limited.

Strikingly, after depletion of endogenous USP11, a significant reduction in PML and SUMO nuclear bodies was observed (**Figure 4A**). Accordingly, depletion of endogenous RNF4 led to significant increases in PML bodies and SUMO bodies. Multiple fields of cells were recorded, and at least 400 cells per experimental condition were quantified, by counting several thousands of nuclear bodies. Ultimately, a 25% reduction in PML bodies and a 50% reduction in SUMO bodies was found upon USP11 depletion, and a 35% increase in PML bodies and a 50% increase in SUMO bodies upon RNF4 depletion (**Figure 4B**). Efficient depletion of both USP11 and RNF4 was confirmed through immunoblot analysis (**Figure 4C**). Similar results were obtained in MCF7 cells (data not shown).

Interestingly, when combining depletion of both USP11 and RNF4, a somewhat intermediate phenotype was observed (**Figure 4A and 4B**). Whereas the increase in PML bodies resulting from depletion of RNF4 was modestly countered by additional knockdown of USP11, there was no clear effect on SUMO positive nuclear bodies. Thus, it is likely that USP11 acts downstream of RNF4, providing an important counterbalancing mechanism to the ubiquitin ligase activity of RNF4 to

of USP11 destabilizes PML and SUMO-2/3 nuclear bodies, whereas depletion of RNF4 stabilizes PML and SUMO-2 nuclear bodies. Scale bars represent 25 μm.
B) Multiple maximum projected fields of cells were recorded as in section A. Cells were counted, and PML and SUMO-2/3 nuclear bodies were quantified per cell. At least 400 cells were counted for each experimental condition, with the exact number of cells shown below each experiment. Error bars represent 2x SEM. Student's t-test p-values are indicated over their respective experiments.
C) Total cell lysates were analyzed by immunoblotting to confirm the depletion of USP11 and RNF4.

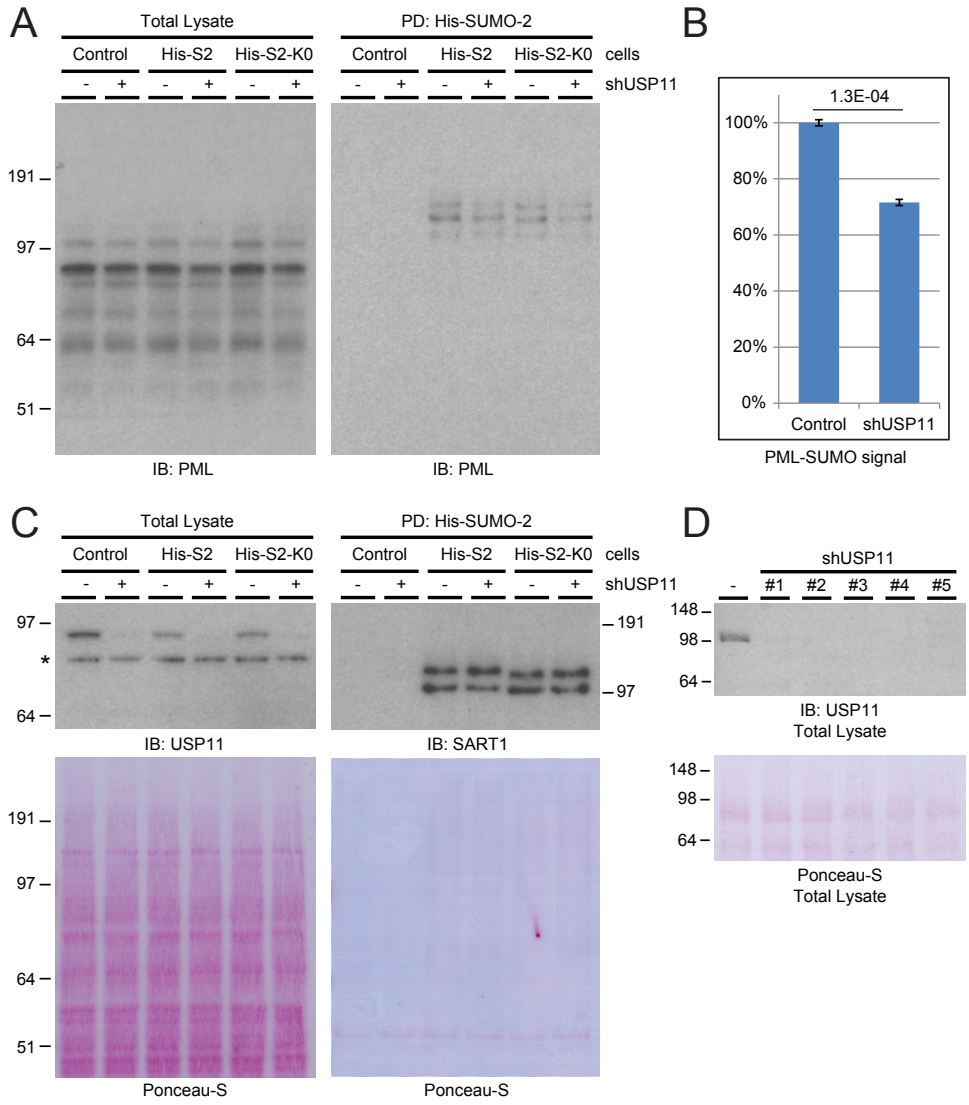

Figure 5. USP11 stabilizes SUMOylated PML.

A) HeLa cells expressing His-tagged SUMO-2, HeLa cells expressing His-tagged lysine-deficient SUMO-2, and parental HeLa cells were either depleted of USP11 by infection with lentiviral knockdown constructs, or treated with an untargeted knockdown construct. After depletion of USP11 cells were lysed, and His-pulldown was performed to enrich SUMOylated proteins. Total lysates and SUMO-enriched fractions were analyzed by immunoblotting using an antibody against PML. Note that PML modified with lysine-deficient SUMO has slightly different migration behavior due to lysine-to-arginine substitutions.

B) Quantification of the PML-SUMO signal in the total lysate and SUMO-enriched lanes corresponding to the His-SUMO cell lines, comparing the PML-SUMO signal in the control versus USP11-depleted cells. Error bars represent standard deviation. Student's t-test p-value is indicated.

establish an important equilibrium characteristic of ubiquitin signaling and generally characteristic for post-translational modifications.

USP11 modulates the level of SUMOylated PML

In addition to cellular analysis by microcopy, the SUMOylation state of the PML protein after depletion of endogenous USP11 in HeLa cells was investigated. In order to facilitate the experiment, HeLa cell lines stably expressing His-tagged SUMO-2 were used to allow for efficient purification of SUMOylated proteins. Additionally, a similar cell line stably expressing lysine-deficient His-tagged SUMO-2 was used in order to investigate a potential effect of inhibited SUMO-2 chain formation on the SUMOylation of PML, and any cumulative result in combination with USP11 depletion. Parental HeLa cells, and the two cell lines expressing the His-tagged SUMO-2 wild-type or lysine-deficient mutant, were all treated with either a lentiviral shRNA targeted against USP11 or a non-targeted shRNA. After depletion of USP11 and enrichment of SUMOylated proteins, total lysates and SUMO-enriched fractions were analyzed by immunoblotting using an antibody against PML (**Figure 5A**).

Similar to observations made with counting PML bodies, a significant decrease in SUMOylated PML was found after depletion of USP11, in both total lysate and SUMO-enriched fractions. Interestingly, in the cell line expressing lysine-deficient SUMO-2, PML was found to be SUMOylated at a somewhat lower base level as compared to the cell line expressing wild-type SUMO-2 (**Figure 5A**). However, a further decrease in SUMOylated PML upon additional USP11 depletion was still observed. Thus, while SUMO-2 deficient in chain-formation reduced the overall levels of SUMOylation on PML, RNF4 was still able to ubiquitylate SUMOylated PML, and USP11 was still able to counteract RNF4 and protect SUMOylated PML from degradation.

The decrease in SUMOylated PML signal was found to be 30% (**Figure 5B**); highly similar to the 25% decrease in PML nuclear bodies observed through confocal microscopy (**Figure 4B**). Efficient depletion of endogenous USP11 was validated by immunoblotting (**Figure 5C and 5D**), and additionally the well-known SUMOylation target protein SART1 [39] was investigated as a control for equal SUMO-enrichment (**Figure 5C**). The SUMOylation state of SART1 was virtually identical regardless of

C) Total lysates from section A were analyzed by immunoblotting with an antibody versus USP11 as a knockdown control, and Ponceau-S staining was used as a loading control. SUMO-enriched fractions from section A were analyzed by immunoblotting with an antibody versus SART1 as a SUMO-level control, and Ponceau-S staining was used as a pulldown control. Note that SART1 modified with lysine-deficient SUMO has slightly different migration behavior due to lysine-to-arginine substitutions.

D) HeLa cells were depleted of USP11 by infection with five different lentiviral knockdown constructs, or treated with an untargeted knockdown construct. Subsequently, cells were lysed, and total lysates were analyzed by immunoblotting using an antibody against USP11. All five viruses were found to be efficient, and a low-concentration mixture of all viruses was used for all other USP11 depletion experiments to provide an effective knockdown.

USP11 depletion, indicating that the effect on PML SUMOylation was specific. Note that the slight shift in migration behavior visible between the wild-type SUMO-2 and the lysine-deficient SUMO-2 is a direct effect of lysine-to-arginine substitutions. Equal total lysate loading and equal pulldown efficiency and loading were confirmed by Ponceau-S staining (**Figure 5C and 5D**).

USP11 prevents the disintegration of nuclear bodies in response to DNA damage

In order to investigate the extent of protection USP11 offers to SUMOylated PML and their associated nuclear bodies, an overexpression experiment was performed where U2-OS cells were transfected with V5-tagged USP11. Subsequently, the cells were treated with MMS, which is known to cause degradation of SUMOylated PML and instigate a disassembly of nuclear bodies [37]. The treatment dose and time chosen for the experiment was sufficient to completely abolish all PML nuclear bodies. Confocal fluorescence microscopy was used to investigate mock treated cells, as well as cells treated with MMS for an extended period of time. Antibodies directed against the V5 tag and against PML were used to detect exogenous V5-USP11 and PML nuclear bodies, respectively. Differential interference contrast (DIC) was used to visualize the nuclei (**Figure 6**).

In untreated cells, nuclear bodies were observed to be distributed fairly equally between cells expressing V5-USP11 and untransfected cells. However, upon MMS treatment, all untransfected cells completely lost their nuclear bodies, whereas many cells overexpressing V5-USP11 were able to retain some PML nuclear bodies, and in some cases these cells even retained all PML bodies (**Figure 6**). Thus, an increased presence of USP11 within the cell was able to counteract the ubiquitylation and degradation of SUMOylated PML, and could counteract the disassembly of the PML nuclear bodies in response to DNA damage.

DISCUSSION

Using a proteomic screen, we have identified USP11 as a ubiquitin protease that co-purified with RNF4, possessing the ability to process hybrid SUMO-ubiquitin polymers. This USP family member contains a DUSP domain with the ability to bind ubiquitin, as well as a catalytic UCH domain. Furthermore, four putative SIMs are harboured between the DUSP and UCH domains. Combined, these domains enabled the processing of hybrid SUMO-ubiquitin chains that were synthesized by RNF4. USP11 was able to deubiquitylate these hybrid chains via its catalytically active C-terminal hydrolase domain. A USP11 mutant lacking the four SIMs between the DUSP domain and the UCH domain was found to be deficient in deubiquitylating hybrid SUMO-ubiquitin chains.

USP11 possesses the ability to counteract RNF4 during regular growth conditions. Depletion of USP11 led to a decrease in the amount of nuclear bodies, whereas depletion of RNF4 led to the exact opposite. Furthermore, we observed

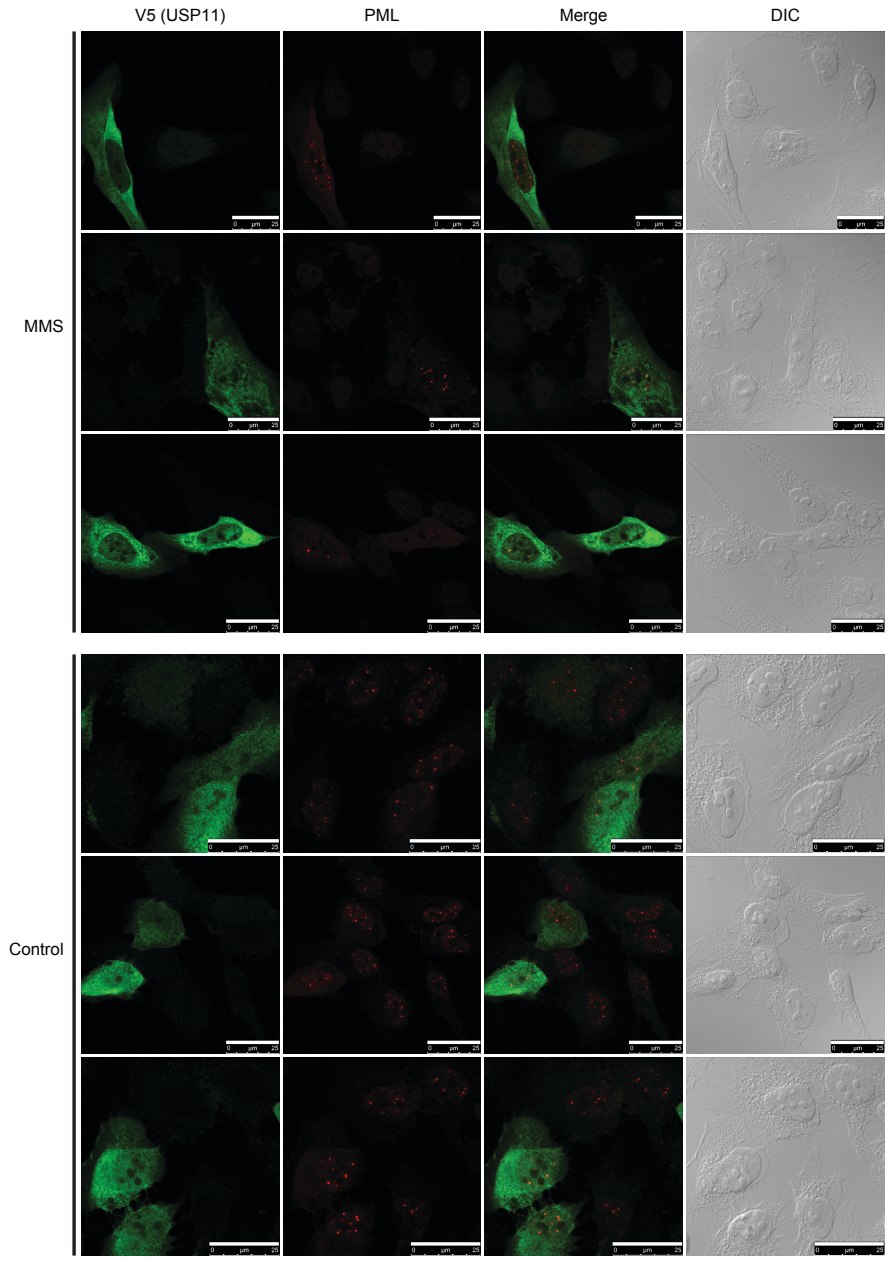

Figure 6. USP11 counteracts RNF4-mediated degradation of nuclear bodies in response to treatment the DNA damaging agent methyl methanesulfonate.
U2OS cells were transfected with a construct encoding V5-USP11, and subsequently mock treated or treated with 0.02% MMS for 135 minutes. Following treatment, cells were fixed, and immunostained. Confocal fluorescence microscopy was used to visualize V5 (USP11 - green) and PML (red). DIC was used to visualize nuclei. Three separate fields of cells are shown for each experimental condition. Upon treatment with MMS, cells overexpressing USP11 retain PML bodies, whereas PML bodies disintegrate in all other cells. Scale bars represent 25 µm.

cells containing a far-above-average amount of PML and SUMO bodies even with the double knockdown, analogous to RNF4-only knockdown (**Figure 4A and 4B**). This could be indicative of USP11 primarily functioning downstream of RNF4. If SUMOylated proteins were not ubiquitylated in the first place, USP11 would logically not have SUMOylated proteins to deubiquitylate. We also noted that USP11 knockdown led to a decrease in the SUMOylated form of PML, indicative of a more rapid degradation through the mechanistic action of RNF4. We did not note a large effect of USP11 on total PML levels overall, as compared to the SUMOylated form (**Figure 5A**).

Moreover, we found that USP11 could counteract RNF4's role in the DNA damage response by blocking the dissociation of PML bodies in response to MMS. We also observed a slight decrease in USP11 levels after MMS treatment in MCF7 cells (**Figure 2B**), suggesting that USP11 may be degraded or otherwise inactivated. The dissociation of PML bodies enables proper progression of the DNA damage response [40] or induction of apoptosis [41, 42].

USP11 was previously found to be involved in repair of double-stranded breaks by homologous recombination, where knockdown of USP11 resulted in spontaneous activation of DNA damage response pathways, rendering cells hypersensitive to PARP inhibition, ionizing radiation and other genotoxic stresses [43]. This finding coincides with our findings, as a loss of PML bodies could prohibit cells from properly responding to DNA damage, and could ambiguously initiate the DNA damage response or cause induction of apoptosis. Similarly, the ability to rescue PML bodies by overexpression of USP11 would thus serve to block the DNA damage response from proceeding efficiently. Furthermore, USP11 has been shown to interact with BRCA2, a key component of the homologous recombination pathway, where BRCA2 was shown to be a target for deubiquitylation by USP11 [44]. Treatment of cells by Mitomycin C led to a degradation of BRCA2, which could be countered by USP11 overexpression, and inhibition of USP11's function increased cellular sensitivity to Mitomycin C [44]. BRCA2 is not known to be SUMOylated. Similar to USP11, RNF4 is also required for homologous recombination [25-27], indicating that balanced ubiquitylation and deubiquitylation of SUMOylated proteins is required for efficient DNA repair via homologous recombination.

The function of USP11 in the DNA damage response makes it a potential clinical target, as inhibition of USP11 would render cancer cells susceptible to apoptosis, especially combined with other treatments such as PARP inhibition. Accordingly, some progress has been made on compounds targeting and counteracting USP11, displaying the ability to inhibit pancreatic cancer cells [45].

More recently, USP11 has been found to interact directly with PML [46]. Contrarily, we found USP11 to interact with the SUMO-targeted ubiquitin ligase RNF4, and a set of SIMs in USP11 potentiated its activity towards hybrid SUMO-ubiquitin chains. Wu et al. further reported that USP11 depletion leads to a decrease in PML bodies, which is consistent with our findings. USP11 overexpression was shown

by Wu et al. to be able to counteract arsenic-induced degradation of PML, but a role in the DNA damage response was not investigated by Wu et al. USP11 was found to be transcriptionally repressed in human glioma, with upregulation of the Hey1/Notch pathway resulting in downregulation of USP11 and correspondingly PML [46]. Interestingly, this was found to increase cellular malignancy as well as potentiate survival and resistance to therapeutic treatment, which is directly opposing findings where antagonizing USP11 leads to inhibition of pancreatic cancer [45], and general findings where USP11 depletion leads to cellular hypersensitivity to DNA damage [43, 44].

We propose that USP11 keeps RNF4 in check, and is able to reverse RNF4's ubiquitylation of SUMOylated proteins (**Figure 4B**). Under certain stress conditions, such as DNA damage, USP11 loses its ability to effectively counteract RNF4, allowing the cellular stress response to proceed efficiently. Thus, our results provide novel insight in crosstalk between SUMOylation and ubiquitylation, and further elucidate the function of USP11 in the DNA damage response.

EXPERIMENTAL PROCEDURES

Plasmids

The cDNA encoding the USP11 protein was a kind gift from Dr. Long Zhang. The cDNA encoding the RNF4 protein was obtained from the Mammalian Gene Collection (Image ID 4824114; supplied by Source Bioscience). Both cDNAs were amplified by a two-step PCR reaction using the following primers: 5'-AAAAAGCAGGCTATATGGCAGTAGCCCCGCGACTG-3' and 5'-AGAAAGCTGGGTGTCAATTAA-CATCCATGAACTC-3' (USP11), 5'-AAAAAGCAGGCTCAATGAGTACAAGAAAGC-3' and 5'-AGAAAGCTGG-GTTTCATATATAAATGG GGTG-3' (RNF4) for the first reaction and 5'- GGGGACAAGTTTGTACAAAAAAG-CAGGCT-3' and 5'-GGGGACCACTTTGTACAAGAAAGCTGGGT-3' for the second reaction. RNF4 was cloned in between the *Spe*I and *Xho*I sites of the plasmid pLV-CMV-X-FLAG-IRES-GFP (kind gift from Dr. R.C. Hoeben). Additionally, RNF4 and USP11 cDNAs were inserted into pDON207 employing standard Gateway technology (Invitrogen). The C318A mutation in USP11 was introduced by QuickChange site-directed mutagenesis (Stratagene) using oligonucleotides 5'-CAATCTGGGCAACACGGCCTTCAT-GAACTCGG-3' and 5'-CCGAGTTCATGAAGGCCGTGTTGCCCAGATTG-3'. pDON207-USP11-C318A-ΔSIMs was generated by a gene synthesis service (GenScript) by replacing residues V183, I184, L186, V197, L199, L200, L201, L202, V203, I259, V261, L262, L271, I272, I273 and M274 with alanines. These different cDNAs were subsequently transferred to the destination vector pDEST-T7-His_6-MBP (a kind gift from Dr. L. Fradkin). RNF4 was cloned into pGEX-2T to obtain a construct encoding GST-tagged RNF4 by amplifying RNF4 cDNA using the following primers: 5'-ACAAACGGATCCATGAGTACAAGAAAGC-GTCGTG-3' and 5'-GCCGCGGAATTCTCATATATAAATGGGGTGGTAC-3'. Both the PCR product and the pGEX-2T vector were subsequently digested with *Bam*HI and *Eco*RI and the PCR product was ligated into the vector with T4 ligase (New England Biolabs). The His_6-ΔN11-SUMO-2-Tetramer expression vector was a kind gift of Prof. Dr. R.T. Hay (Dundee, U.K.) [21].

Cell culture & cell line generation

MCF7, U2-OS and HeLa cells were cultured in Dulbecco's Modified Eagle's Medium (DMEM) supplemented with 10% FBS and 100 U/mL penicillin and streptomycin (Invitrogen). MCF7 cells stably expressing RNF4-FLAG were generated through lentiviral infection with a construct carrying RNF4-FLAG-IRES-GFP. The Internal Ribosome Entry Site (IRES) allowed the same mRNA to code for a non-fused GFP, in order to quantify RNF4-FLAG expression without adding a bulky fusion tag to RNF4. Similarly, MCF7 and HeLa cell lines stably expressing His-SUMO-2 were generated through lentiviral

infection with a construct encoding His-SUMO-2-IRES-GFP. Two weeks after infection, cells were sorted for a low level of GFP by flow cytometry, using a FACSAria II (BD Biosciences).

Treatments, transfection and lentiviral infection

Cells were treated with 0.02% MMS and 1 μM As_2O_3 (Sigma) for the indicated amounts of time. For transfection, cells were cultured in DMEM lacking penicillin and streptomycin. Transfections were performed using 2.5 μg of polyethylenimine (PEI) per 1 μg of plasmid DNA, using 1 μg of DNA per 1 million cells. Transfection reagents were mixed in 150 mL NaCl and allowed to rest for 15 minutes before adding it directly to the cells. Cells were split after 24 hours (if applicable) and investigated after 48 hours. Lentiviruses were generated essentially as described previously [47]. Infections were performed with a multiplicity of infection of 2 and using a concentration of 8 μg/mL polybrene in the medium. 24 hours after infection the medium was replaced. Cells were split 72 hours after infection (if applicable) and investigated 96 hours after infection.

RNF4-FLAG purification

Parental MCF7 cells and MCF7 cells stably expressing RNF4-FLAG were grown in regular DMEM, until fully confluent in 10x 15-cm dishes (approximately 0.2 billion cells). Cells were washed 3 times in ice-cold PBS prior to addition of 3 mL of ice-cold Lysis Buffer to each plate (150 mM NaCl, 50 mM TRIS, 0.5% sodium deoxycholate, 1.0% N-P40, buffered at pH 7.5, with every 10 mL of Lysis Buffer supplemented by one tablet of protease inhibitors + EDTA (Roche)). Subsequently, cells were scraped in the Lysis Buffer, on ice, and collected in 50 mL tubes. The lysates were sonicated on ice for 10 seconds using a microtip sonicator at 30 Watts. Next, lysates were centrifuged at 4 °C and 10,000 RCF to clear debris from the soluble fraction. Lysates were equalized using the bicinchoninic acid assay (BCA, Pierce). 1 μL (dry volume) of FLAG-M2 agarose beads (Sigma) were prepared per 1 mL of lysate, and equilibrated by washing 5 times in ice-cold Lysis Buffer. FLAG-M2 beads were added to the lysates and incubated while tumbling for 2 hours at 4 °C. Next, beads were pelleted by centrifugation at 250 RCF and washed 5 times with ice-cold Lysis Buffer. After every single wash step, the tubes were exchanged. RNF4-FLAG and interacting proteins were eluted off the beads by incubating them for 10 minutes with three bead volumes of Lysis Buffer supplemented with 1 mM FLAG-M2 peptide. Elution of the beads was repeated twice, and a fourth elution was performed with 2x LDS Sample Buffer (Novex). The primary three peptide elutions were pooled and concentrated. Culturing of cells, immunoprecipitation of RNF4-FLAG and subsequent steps leading to the LC-MS/MS analysis were performed in biological triplicate.

Purification of His-SUMO-2

Purification of His-SUMO-2-modified proteins was essentially performed as described previously [8].

Recombinant proteins

His_6-MBP and His_6-ΔN11-SUMO-2-Tetramer recombinant proteins were purified essentially as described previously [39]. Briefly, BL21 cells were transformed with expression constructs. Cells were grown to an OD600 of 0.6. Subsequently, cells were grown overnight at 24°C in the presence of 0.1 mM isopropyl-β-D-thiogalactopyranoside (IPTG), 20 mM HEPES pH 7.5, 1 mM $MgCl_2$ and 0.05% Glucose. Lysates were prepared and proteins were affinity-purified on TALON beads (BD Biosciences). GST-tagged RNF4 was produced in *E. coli* and purified as described previously [48].

***In vitro* ubiquitylation and deubiquitylation assay**

15 ng of His_6-ΔN11-SUMO-2-Tetramer was *in vitro* ubiquitylated using 8 μM ubiquitin, 40 nM UBE1, 0.7 μM UbcH5a (all from Boston Biochem), 0.5 μM GST-RNF4 in 50 mM TRIS pH 7.5, 5 mM $MgCl_2$, 1 mM DTT, and 4 mM ATP. 5 μL reactions were incubated at 37°C for three hours after which different concentrations (1 to 7.5 μg) of His_6-MBP-USP11 proteins were added to a final volume of 15 μL. Reaction were incubated at 37°C for an additional three hours. Finally, reactions were stopped by adding 5 μL 4X LDS Sample Buffer (Novex).

***In vitro* interaction assay**

In vitro ubiquitylation reactions were performed as described above in the presence or absence of 250 ng His_6-ΔN11-SUMO-2-Tetramer. Ubiquitin or SUMO-2-Ubiquitin chains were incubated with 5 µg His_6-MBP-RNF4, His_6-MBP-USP11-C318A, His_6-MBP-USP11-ΔSIMs-C318A or His_6-MBP elution buffer in EBC buffer (50 mM TRIS pH 7.5, 150 mM NaCl, 1 mM EDTA, 1 mM DTT, 0.5 % NP-40) [23]. Reactions were incubated at 4°C for 2 hours, and subsequently bound to 25 µL of Amylose resin (New England Biolabs) for another 2 hours at 4°C. Beads were washed extensively with EBC buffer and finally eluted in 25 µL 2X LDS sample buffer.

Electrophoresis and immunoblotting

Protein samples were size-fractioned on Novex 4-12% Bis-Tris gradient gels using MOPS as a running buffer (Invitrogen), or on regular SDS-PAGE gels with a Tris-Glycine running buffer. Size-separated proteins were transferred to Hybond-C membranes (Amersham Biosciences) using a submarine system (Invitrogen). Membranes were stained for total protein loading using Ponceau-S (Sigma). Membranes were blocked using PBS containing 0.1% Tween-20 (PBST) and 5% milk powder for one hour. Subsequently, membranes were incubated with primary antibodies as indicated, in blocking solution. Incubation with primary antibody was performed overnight at 4 °C. Subsequently, membranes were washed three times with PBST and briefly blocked again with blocking solution. Next, membranes were incubated with secondary antibodies (donkey-anti-mouse-HRP or rabbit-anti-goat-HRP) for one hour, before washing three times with PBST and two times with PBS. Membranes were then treated with ECL2 (Pierce) as per manufacturer's instructions, and chemiluminescence was captured using Biomax XAR film (Kodak).

Antibodies

The following antibodies were used in this study: mouse α FLAG (M2, Sigma), mouse α PML (5E10, kind gift from Prof. R. van Driel, University of Amsterdam [49]), rabbit α USP11 (A301-613A, Bethyl), mouse α SUMO-2/3 (8A2, Abcam), rabbit α SUMO-2/3 (raised against the C-terminus of SUMO-2), rabbit α RNF4 (raised against GST-RNF4), rabbit α SART1 (raised against GST-SART1), rabbit α V5 (V8137, Sigma), mouse α His (HIS-1, Sigma) and rabbit α Ubiquitin (9133, Santa Cruz).

Electrophoresis, Coomassie Staining and In-gel digestion

RNF4-FLAG IP samples were size-separated by SDS-PAGE using Novex 4-12% gradient gels and MES SDS running buffer (Invitrogen), followed by staining with Colloidal Blue Kit (Invitrogen). Gel lanes were excised as ten slices per eluted fraction, cut into 2-mm^3 cubes and in-gel digested with sequencing-grade modified trypsin (Promega) as described before (Shevchenko et al., 2006). The peptides extracted from the gel after digestion were cleaned, desalted and concentrated on C18 reverse phase StageTips [50].

LC-MS/MS analysis and data processing

Experiments were performed in triplicate. The analysis of in-gel digested samples was performed as described previously (Schimmel et al. 2014, in press). Raw data were processed using MaxQuant [51, 52]. RNF4-FLAG interactors were investigated through inspection of Label-Free Quantification (LFQ) intensities as well as MS/MS spectral counting.

Microscopy

Cells were seeded on glass coverslips, and fixed 24 hours later for 10 minutes in 3.7% paraformaldehyde in PHEM buffer (60 mM PIPES, 25 mM HEPES, 10 mM EGTA, 2 mM MgCl2 pH 6.9) at 37 °C. After washing with PBS, cells were permeated with 0.1% Triton-X100 for 10 minutes, washed with PBST, and blocked using TNB (100 mM TRIS pH 7.5, 150 mM NaCl, 0.5% Blocking Reagent (Roche)) for 30 minutes. Cells were incubated with primary antibody as indicated, in TNB for one hour. Subsequently cells were washed five times with PBST, and incubated with secondary antibodies (Goat α Ms Alexa 488 and Goat α Rb Alexa 594 (Invitrogen)) in TNB for one hour. Next, cells were washed five times

with PBST and dehydrated using alcohol, prior to fixing them in DAPI solution (Citifluor) and sealing the slides with nail varnish. Images were recorded on a Leica SP5 confocal microscope system using 488 nm and 561 nm lasers for excitation, a 63X lens for magnification, and were analyzed with Leica confocal software. For quantification of PML bodies, groups of cells were recorded in similar-sized fields using Z-stacking with steps of 0.5 µm to acquire 10 images ranging from the bottom to the top of the cells. Images were maximum projected, individual cells were localized and PML bodies were counted using in-house customized Stacks software [53].

Structural modeling of USP11

The structure of USP11 was modeled using the Protein Homology/analogY Recognition Engine V 2.0 (PHYRE2)[38]. *Homo sapiens* USP11 (Uniprot ID P51784) was submitted to the PHYRE2 Protein Fold Recognition Server, and subjected to Intensive Modelling. 3D Molecule Viewer (Vector NTI Advance 11.5.1, Invitrogen), was used to highlight putative SIMs within the structure.

ACKNOWLEDGMENTS

We are grateful to Drs. R. van Driel, R.T. Hay, R.C. Hoeben and L. Fradkin for providing critical reagents and to M. Verlaan – de Vries for technical assistance. This work was supported by the Netherlands Organization for Scientific Research (NWO) (A.C.O.V.), ZonMW (A.C.O.V.), the European Research Council (A.C.O.V) and the research career program FSS Sapere Aude (J.V.O.) from the Danish Research Council. The NNF Center for Protein Research is supported by a generous donation from the Novo Nordisk Foundation.

Reference List

1. Flotho, A., and Melchior, F. (2013) Sumoylation: a regulatory protein modification in health and disease. *Annu. Rev. Biochem.* 82, 357-385
2. Hickey, C. M., Wilson, N. R., and Hochstrasser, M. (2012) Function and regulation of SUMO proteases. *Nat. Rev. Mol. Cell Biol.* 13, 755-766
3. Hay, R. T. (2007) SUMO-specific proteases: a twist in the tail. *Trends Cell Biol.* 17, 370-376
4. Nacerddine, K. et al. (2005) The SUMO pathway is essential for nuclear integrity and chromosome segregation in mice. *Dev. Cell* 9, 769-779
5. Becker, J. et al. (2013) Detecting endogenous SUMO targets in mammalian cells and tissues. *Nat. Struct. Mol. Biol.* 20, 525-531
6. Golebiowski, F. et al. (2009) System-wide changes to SUMO modifications in response to heat shock. *Sci. Signal.* 2, ra24
7. Vertegaal, A. C. (2011) Uncovering ubiquitin and ubiquitin-like signaling networks. *Chem. Rev.* 111, 7923-7940
8. Matic, I. et al. (2010) Site-specific identification of SUMO-2 targets in cells reveals an inverted SUMOylation motif and a hydrophobic cluster SUMOylation motif. *Mol. Cell* 39, 641-652
9. Rodriguez, M. S., Dargemont, C., and Hay, R. T. (2001) SUMO-1 conjugation in vivo requires both a consensus modification motif and nuclear targeting. *J. Biol. Chem.* 276, 12654-12659
10. Bernier-Villamor, V., Sampson, D. A., Matunis, M. J., and Lima, C. D. (2002) Structural basis for E2-mediated SUMO

conjugation revealed by a complex between ubiquitin-conjugating enzyme Ubc9 and RanGAP1. *Cell* 108, 345-356

11. Kerscher, O. (2007) SUMO junction-what's your function? New insights through SUMO-interacting motifs. *EMBO Rep.* 8, 550-555
12. Danielsen, J. R. et al. (2012) DNA damage-inducible SUMOylation of HERC2 promotes RNF8 binding via a novel SUMO-binding Zinc finger. *J. Cell Biol.* 197, 179-187
13. Hunter, T., and Sun, H. (2008) Crosstalk between the SUMO and ubiquitin pathways. *Ernst. Schering. Found. Symp. Proc.*, 1-16
14. Ulrich, H. D. (2005) Mutual interactions between the SUMO and ubiquitin systems: a plea of no contest. *Trends Cell Biol.* 15, 525-532
15. Desterro, J. M., Rodriguez, M. S., and Hay, R. T. (1998) SUMO-1 modification of Ikappa-Balpha inhibits NF-kappaB activation. *Mol. Cell* 2, 233-239
16. Huang, T. T., Wuerzberger-Davis, S. M., Wu, Z. H., and Miyamoto, S. (2003) Sequential modification of NEMO/IKKgamma by SUMO-1 and ubiquitin mediates NF-kappaB activation by genotoxic stress. *Cell* 115, 565-576
17. Schimmel, J. et al. (2008) The ubiquitin-proteasome system is a key component of the SUMO-2/3 cycle. *Mol. Cell Proteomics* 7, 2107-2122
18. Tatham, M. H., Matic, I., Mann, M., and Hay, R. T. (2011) Comparative proteomic analysis identifies a role for SUMO in protein quality control. *Sci. Signal.* 4, rs4
19. Prudden, J. et al. (2007) SUMO-targeted ubiquitin ligases in genome stability. *EMBO J.* 26, 4089-4101
20. Sun, H., Leverson, J. D., and Hunter, T. (2007) Conserved function of RNF4 family proteins in eukaryotes: targeting a ubiquitin ligase to SUMOylated proteins. *EMBO J.* 26, 4102-4112
21. Tatham, M. H. et al. (2008) RNF4 is a poly-SUMO-specific E3 ubiquitin ligase required for arsenic-induced PML degradation. *Nat. Cell Biol.* 10, 538-546
22. Sun, H., and Hunter, T. (2012) Poly-small ubiquitin-like modifier (PolySUMO)-binding proteins identified through a string search. *J. Biol. Chem.* 287, 42071-42083
23. Poulsen, S. L. et al. (2013) RNF111/Arkadia is a SUMO-targeted ubiquitin ligase that facilitates the DNA damage response. *J. Cell Biol.* 201, 797-807
24. Heideker, J., Perry, J. J., and Boddy, M. N. (2009) Genome stability roles of SUMO-targeted ubiquitin ligases. *DNA Repair (Amst)* 8, 517-524
25. Yin, Y. et al. (2012) SUMO-targeted ubiquitin E3 ligase RNF4 is required for the response of human cells to DNA damage. *Genes Dev.* 26, 1196-1208
26. Galanty, Y., Belotserkovskaya, R., Coates, J., and Jackson, S. P. (2012) RNF4, a SUMO-targeted ubiquitin E3 ligase, promotes DNA double-strand break repair. *Genes Dev.* 26, 1179-1195
27. Vyas, R. et al. (2013) RNF4 is required for DNA double-strand break repair in vivo. *Cell Death Differ.* 20, 490-502
28. Luo, K., Zhang, H., Wang, L., Yuan, J., and Lou, Z. (2012) Sumoylation of MDC1 is important for proper DNA damage response. *EMBO J.* 31, 3008-3019
29. van, H. M., Overmeer, R. M., Abolvardi, S. S., and Vertegaal, A. C. (2010) RNF4 and VHL regulate the proteasomal degradation of SUMO-conjugated Hypoxia-Inducible Factor-2alpha. *Nucleic Acids Res.* 38, 1922-1931
30. Hu, X. V. et al. (2010) Identification of RING finger protein 4 (RNF4) as a modulator of DNA demethylation through a functional

genomics screen. *Proc. Natl. Acad. Sci. U. S. A* 107, 15087-15092
31. Nijman, S. M. et al. (2005) A genomic and functional inventory of deubiquitinating enzymes. *Cell* 123, 773-786
32. Reyes-Turcu, F. E., Ventii, K. H., and Wilkinson, K. D. (2009) Regulation and cellular roles of ubiquitin-specific deubiquitinating enzymes. *Annu. Rev. Biochem.* 78, 363-397
33. Lin, D. Y. et al. (2006) Role of SUMO-interacting motif in Daxx SUMO modification, subnuclear localization, and repression of sumoylated transcription factors. *Mol. Cell* 24, 341-354
34. Weisshaar, S. R. et al. (2008) Arsenic trioxide stimulates SUMO-2/3 modification leading to RNF4-dependent proteolytic targeting of PML. *FEBS Lett.* 582, 3174-3178
35. Lallemand-Breitenbach, V. et al. (2008) Arsenic degrades PML or PML-RARalpha through a SUMO-triggered RNF4/ubiquitin-mediated pathway. *Nat. Cell Biol.* 10, 547-555
36. Bruderer, R. et al. (2011) Purification and identification of endogenous polySUMO conjugates. *EMBO Rep.* 12, 142-148
37. Conlan, L. A., McNees, C. J., and Heierhorst, J. (2004) Proteasome-dependent dispersal of PML nuclear bodies in response to alkylating DNA damage. *Oncogene* 23, 307-310
38. Kelley, L. A., and Sternberg, M. J. (2009) Protein structure prediction on the Web: a case study using the Phyre server. *Nat. Protoc.* 4, 363-371
39. Schimmel, J. et al. (2010) Positively charged amino acids flanking a sumoylation consensus tetramer on the 110kDa tri-snRNP component SART1 enhance sumoylation efficiency. *J. Proteomics* 73, 1523-1534
40. Dellaire, G., and Bazett-Jones, D. P. (2004) PML nuclear bodies: dynamic sensors of DNA damage and cellular stress. *Bioessays* 26, 963-977
41. Guo, A. et al. (2000) The function of PML in p53-dependent apoptosis. *Nat. Cell Biol.* 2, 730-736
42. Wang, Z. G. et al. (1998) PML is essential for multiple apoptotic pathways. *Nat. Genet.* 20, 266-272
43. Wiltshire, T. D. et al. (2010) Sensitivity to poly(ADP-ribose) polymerase (PARP) inhibition identifies ubiquitin-specific peptidase 11 (USP11) as a regulator of DNA double-strand break repair. *J. Biol. Chem.* 285, 14565-14571
44. Schoenfeld, A. R., Apgar, S., Dolios, G., Wang, R., and Aaronson, S. A. (2004) BRCA2 is ubiquitinated in vivo and interacts with USP11, a deubiquitinating enzyme that exhibits prosurvival function in the cellular response to DNA damage. *Mol. Cell Biol.* 24, 7444-7455
45. Burkhart, R. A. et al. (2013) Mitoxantrone Targets Human Ubiquitin-Specific Peptidase 11 (USP11) and Is a Potent Inhibitor of Pancreatic Cancer Cell Survival. *Mol. Cancer Res.* 11, 901-911
46. Wu, H. C. et al. (2014) USP11 regulates PML stability to control Notch-induced malignancy in brain tumours. *Nat. Commun.* 5, 3214
47. Tiscornia, G., Singer, O., and Verma, I. M. (2006) Production and purification of lentiviral vectors. *Nat. Protoc.* 1, 241-245
48. Tatham, M. H. et al. (2001) Polymeric chains of SUMO-2 and SUMO-3 are conjugated to protein substrates by SAE1/SAE2 and Ubc9. *J. Biol. Chem.* 276, 35368-35374
49. Stuurman, N. et al. (1992) A monoclonal antibody recognizing nuclear matrix-associated nuclear bodies. *J. Cell Sci.* 101 (Pt 4),

773-784

50. Rappsilber, J., Mann, M., and Ishihama, Y. (2007) Protocol for micro-purification, enrichment, pre-fractionation and storage of peptides for proteomics using StageTips. *Nat. Protoc.* 2, 1896-1906
51. Cox, J. et al. (2011) Andromeda: a peptide search engine integrated into the MaxQuant environment. *J. Proteome. Res.* 10, 1794-1805
52. Cox, J., and Mann, M. (2008) MaxQuant enables high peptide identification rates, individualized p.p.b.-range mass accuracies and proteome-wide protein quantification. *Nat. Biotechnol.* 26, 1367-1372
53. Smeenk, G. et al. (2010) The NuRD chromatin-remodeling complex regulates signaling and repair of DNA damage. *J. Cell Biol.* 190, 741-749

A

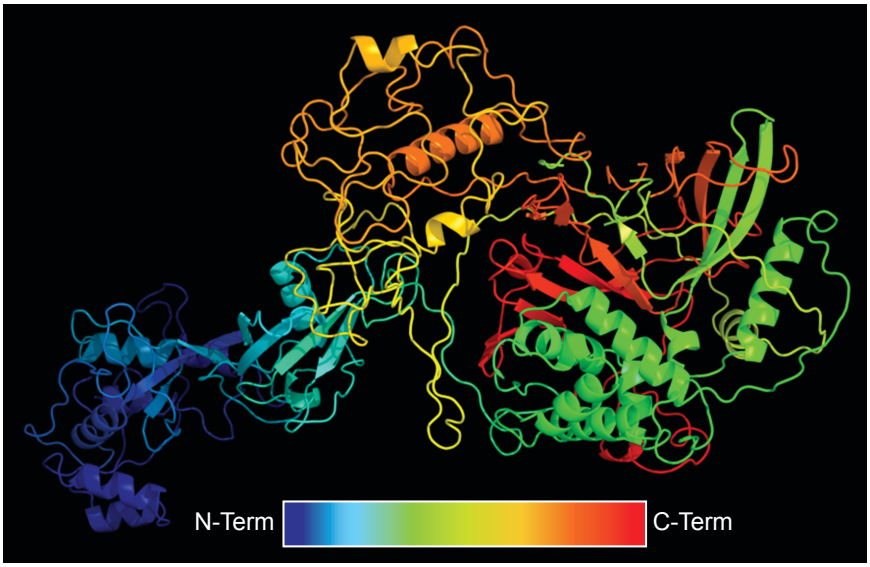
N-Term
C-Term

B


76
184
309
931
N-term (1)
DUSP
UCH
(963) C-Term
Potential SIMs

C

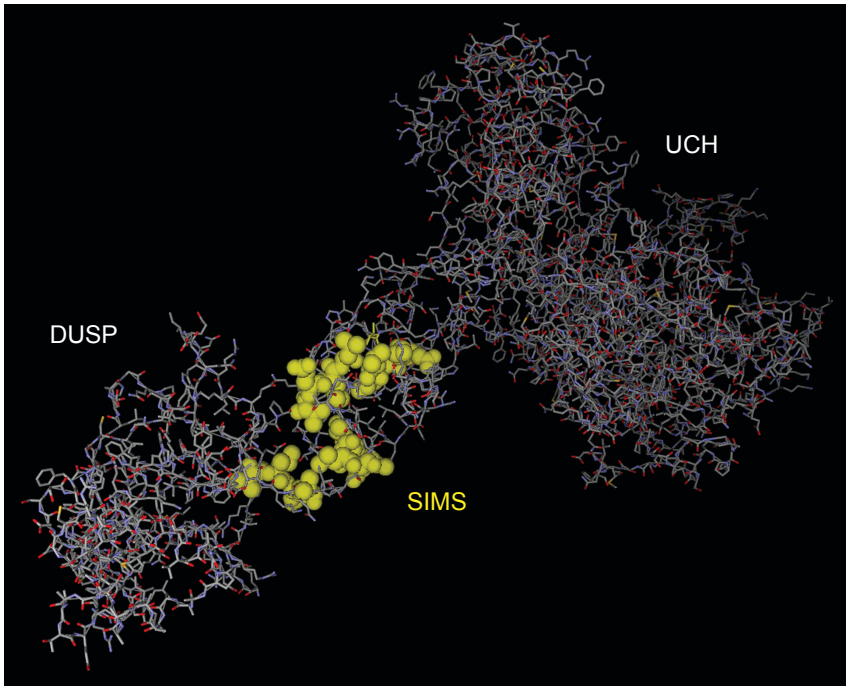
UCH
DUSP
SIMS

Figure S1. Structural modeling of USP11 reveals four putative SIMs to be located within the DUSP and UCH domains.

A) A rainbow-ribbon model of USP11, using a gradual transition in color to indicate progression from N-terminus to C-terminus. Alpha helices and beta sheets are indicated.

B) Cartoon depicting USP11. USP11 harbors a Domain present in Ubiquitin-Specific Proteases (DUSP) and an Ubiquitin Carboxyl-terminal Hydrolase domain (UCH). USP11 contains four potential SUMO interacting motifs (SIMs), located in between the DUSP and UCH domains.

C) A structural skeleton model of USP11, with the SIMs indicated in yellow and using space-fill modelling for the respective molecules. The general location of the DUSP, UCH and SIMs are indicated.